

Crystallization of amorphous Te-20 at.% Pb alloy obtained by rapid cooling from the liquid state

M. KACZOROWSKI, J. KOZUBOWSKI, B. DABROWSKI, H. MATYJA
*Institute of Materials Science and Engineering, Warsaw Technical University, Narbutta 85,
02-524 Warsaw, Poland*

Crystallization of amorphous Te-20 at. % Pb alloy obtained by rapid cooling from the liquid state was investigated by differential thermal analysis, X-ray diffraction and transmission electron microscopy. It was found that crystallization, beginning at 337 K, is of a continuous nature and proceeds over a fairly wide temperature range. At the first crystallization stage, nucleation of the metastable phase MS I, with hexagonal structure and lattice parameters $a = 4.49 \text{ \AA}$ and $c = 5.85 \text{ \AA}$, takes place. Contrasts observed in the micrographs of single crystals of phase MS I were interpreted as areas with increased concentration of Pb atoms. With rising temperature, the phase present in these areas dissolves, and in its place platelet precipitates of the compound PbTe appear. In this paper, a sequence of decomposition for the amorphous phase obtained in the Te-20 at. % Pb alloy, as well as a model for the precipitation of PbTe, are proposed.

1. Introduction

Tellurium alloys belong to some of the first to be obtained in amorphous state by rapid cooling of liquid [1]. Since they exhibit interesting physical properties from both practical and theoretical standpoints, they have been extensively studied of late [2-6]. However, no detailed studies of the crystallization process of amorphous Te alloys, except for alloys of the Ge-Te system [7, 8] have so far been reported.

The objective of the present study was to observe the phase transitions taking place in Te-20 at. % Pb alloy rapidly cooled from the liquid state, during continuous heating, with special consideration of the sequence of these transitions. Moreover, we were interested in the stability of the amorphous phase, which is closely related to the temperature of crystallization T_x . It was also intended to determine whether the crystallization mechanism involves nucleation and growth, or only growth, of microcrystals. Furthermore, it was resolved to establish the structure of metastable intermediate phases, if formed. The experimental

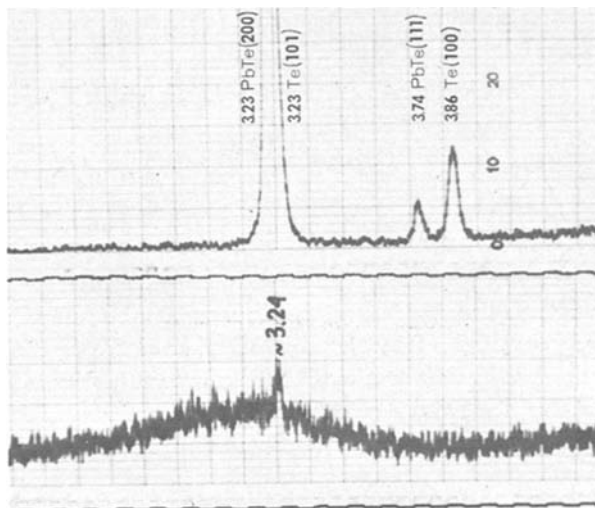
techniques employed in this study comprised differential thermal analysis (DSC), X-ray diffraction and transmission electron microscopy (TEM) combined with microdiffraction (SAD).

2. Experimental

Te-20 at. % Pb alloy was prepared from materials of very high purity (99.999%). Alloy components (total weight 10 g) were sealed in a quartz ampoule under a vacuum of 10^{-5} torr, and melted at a temperature exceeding the liquidus temperature by 100 K. To ensure homogeneity of the alloy composition, melting was repeated several times with stirring of the alloy. Each melting lasted 0.5 h. Thin foils were obtained by the gun method as described by Duwez and Willens [9]. Copper and silver of 99.99% purity were used as substrates.

The structure of the alloy after rapid cooling was examined diffractometrically and microscopically. Diffractometric examinations were carried out on a Philips PM 8000 diffractometer, using $\text{CoK}\alpha$ radiation; microscopic observations were made in a Philips EM 300 transmission electron

Figure 1 Comparison of X-ray diffraction patterns for equilibrium and as-quenched Te–20 at. %Pb alloy.



microscope operating at an accelerating voltage of 100 kV.

Crystallization of the alloy was examined under conditions of continuous heating at constant rate up to definite temperatures established on the basis of the results of DSC studies. Calorimetric measurements were taken in a Perkin–Elmer DSC-2 differential microcalorimeter, at a heating rate of 20 K min^{-1} . Structures of the phases formed during crystallization were identified by X-ray diffraction and electron diffraction. Specimens used in these studies were heated under argon at a rate of 5 K min^{-1} . The heating rate of foils intended for TEM studies was lower, because only then were the resulting crystals sufficiently large to permit growth morphology observation and application of SAD. Microscopic studies were performed by two methods. The first method was aimed at recording the structural and morphological changes in foils heated outside the TEM; the second method involved continuous observation of the phase transitions initiated by electron-beam heating. To this end, some foils were first heated in a microcalorimeter to the temperature of the beginning of crystallization T_x and subsequently placed inside the TEM (some foils were introduced into TEM immediately after rapid cooling). The foils inside the TEM were then heated by electron beam till the equilibrium structure of the alloy was attained. The most characteristic stages of the transition were recorded in micrographs and diffraction patterns.

On account of the structural and morphological similarities between the crystals obtained as a

result of heating either outside or inside TEM, the results obtained by the second method are presented in this paper.

3. Results

3.1. Structure of alloy after rapid cooling

Fig. 1 presents part of an X-ray diffractogram obtained for a Te–20 at. %Pb alloy immediately after rapid cooling. The diffuse maximum characteristic of materials exhibiting at most a short-range order in the diffractogram. If it is assumed that the structure of the alloy is microcrystalline, then the hypothetical size of microcrystals, calculated from Scherrer's formula, would be $\sim 15\text{ \AA}$. In addition to the diffuse maximum, a faint reflection originating from the crystalline phase is visible; this indicates that the alloy has not been obtained in non-crystalline (amorphous) state in its whole volume.

Figs. 2a and b present the electron micrographs of the structure of the alloy after rapid cooling, as observed by TEM, in bright and dark fields. The bright-field picture (Fig. 2a) indicates that the alloy shows no crystalline structure. This fact is confirmed by the diffraction pattern (inset of Fig. 2a) showing diffuse rings analogous to the diffuse maximum in the X-ray diffractogram (Fig. 1). To obtain a picture in the dark field, a part of the first diffuse ring was used with application of the method of beam inclination; this part is marked with a circle in the diffraction pattern. Dark field observations point to the presence of coherently scattering regions (15 to 20 \AA across) analogous to those observed by Chaudhari *et al.* [10], as well as

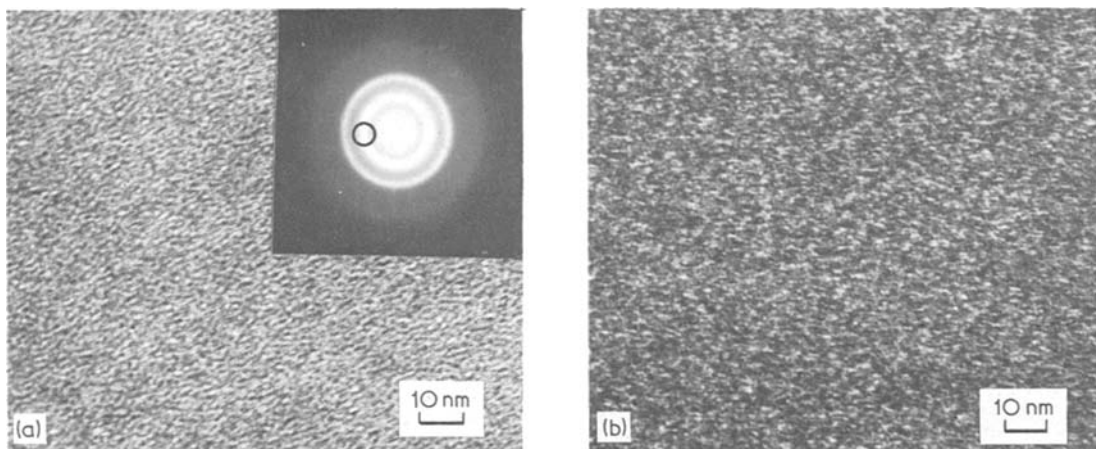


Figure 2 (a) TEM bright-field micrograph and diffraction pattern of as-quenched foil. (b) Dark-field of the same area.

by Herd and Chaudhari [11] in Te–Ge, Pd–Si and Au–Ni alloys. Consistent with the suggestions of the above authors, the occurrence in dark-field pictures of contrasts similar to those given by the coherently scattering regions is not necessarily a proof of the microcrystalline structure of the alloy, contrary to the opinions of Rudee [12] as well as of Howie *et al.* [13], who have tried to demonstrate the opposite.

3.2. Annealing behaviour

The thermogram of as-quenched Te–20 at. % Pb alloy is shown in Fig. 3. The first exothermic effect found in the DSC curve is related to the nucleation of the crystalline phase, beginning at 337 K. Unfortunately, the second very small thermal effect could not be identified. The third

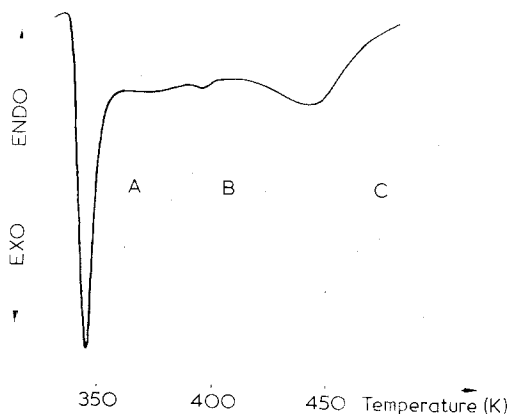


Figure 3 DSC curves (scanning rate 20 deg min⁻¹). A, B, C denotes temperatures to which samples were heated in order to study structural transformations in splat-cooled Te–20 at. % Pb alloy.

thermal effect observed within the range 414 to 550 K is associated with precipitation processes. The course of the DSC curve between the end of the first and the beginning of the third transition clearly testifies to the continuous nature of the transition from the amorphous to the crystalline state; this is confirmed by the fact that within the above-mentioned temperature range the DSC curve does not attain the line of the base. The above statement was fully confirmed by the subsequently performed X-ray diffractometric and microscopic studies.

3.3. X-ray diffraction

Diffractometric studies were performed using samples heated according to the schema presented in Fig. 3. These studies demonstrate that the metastable phase with hexagonal structure and lattice parameters $a = 4.49 \text{ \AA}$ and $c = 5.85 \text{ \AA}$ is the first one to be formed. This phase, designated by the symbol MS I, is most probably a solid solution of Te(Pb), in which the lead atoms are distributed at random within the Te chains. The fact that, after heating of the alloy to the temperature of the end of the first transition and maintaining it at this temperature for 30 sec, the diffuse maximum originating from the amorphous phase is still present in the diffractogram, is important; it confirms the assumption of the continuous nature of the decomposition of the amorphous phase, as deduced from the calorimetric data. Moreover, it is of importance that the phase MS I crystallizing in the amorphous matrix probably exhibits the same structure as the crystalline phase which is formed in addition to the amorphous phase as a result of

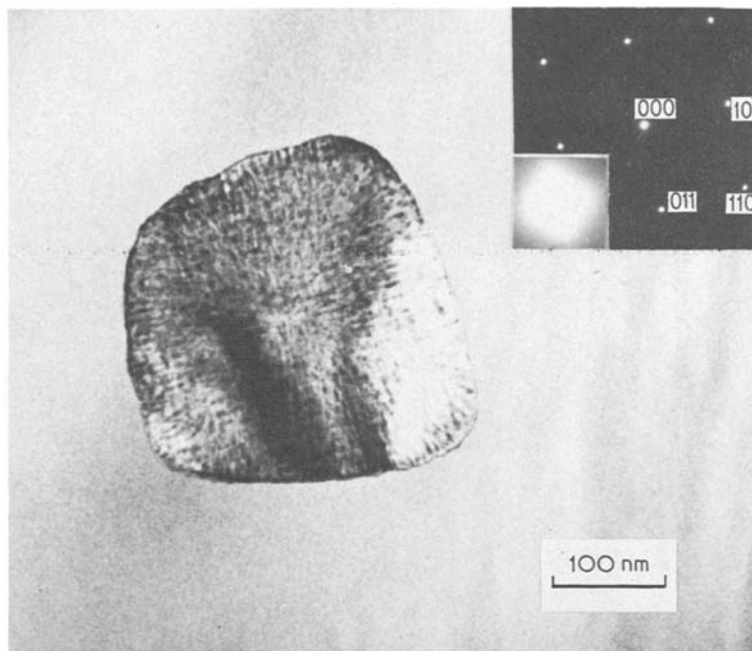


Figure 4 TEM micrograph of single crystal in amorphous matrix after heating of alloy up to 337 K. Diffraction pattern is shown in right upper corner, together with one of the spots magnified ~ 15 times.

rapid cooling from liquid state (Fig. 1). This conclusion is based on the facts that during alloy crystallization the initially faint reflection originating from the crystalline phase gradually increases (Fig. 1), and that there are no diffraction lines which could not be assigned to the metastable intermediate phase MS I.

Diffractograms obtained for the samples heated to higher temperatures (treatments B and C in Fig. 3) show that the compound PbTe precipitates in these specimens, with resulting attainment of the equilibrium structure of the alloy.

3.4. Electron microscopy

Fig. 4 shows a single crystal in the amorphous matrix, formed during foil heating outside the TEM. Contrasts occurring in two almost perpendicular directions are observed in the crystal. The picture in the corner shows the electron diffraction pattern of this crystal. One of the diffraction spots, magnified about 15 times, is presented in the insert; the picture shows the characteristic distribution of the intensity, which can be due to the occurrence of satellite reflections around the main one. During electron-beam heating the crystal grows (Fig. 5), this growth being associated with a sharpening of the contrasts in the micrographs, as well as an increased diffuseness of the reflections

in the diffraction patterns (Fig. 6a and b). Upon further heating of the foil the contrasts disappear and simultaneously platelet precipitation occurs, to subsequently undergo coagulation (Fig. 7a and b). The increase in the platelet precipitation, which according to the interpretation of the diffraction patterns involves the compound PbTe, is associated with a loss of coherence; this is proved, *inter alia*, by dislocations occurring at the interphase boundary (Fig. 7b).

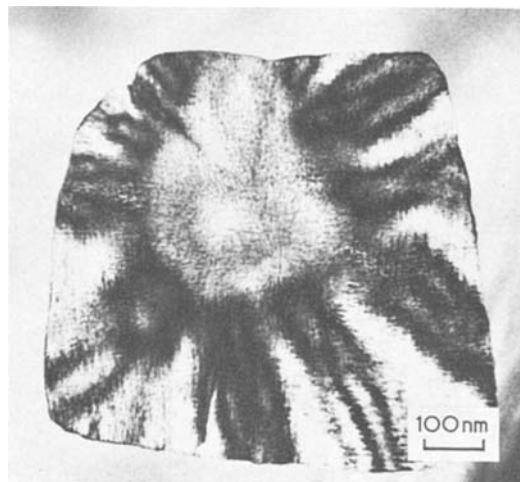


Figure 5 The same crystal as shown in Fig. 4, after further beam heating.

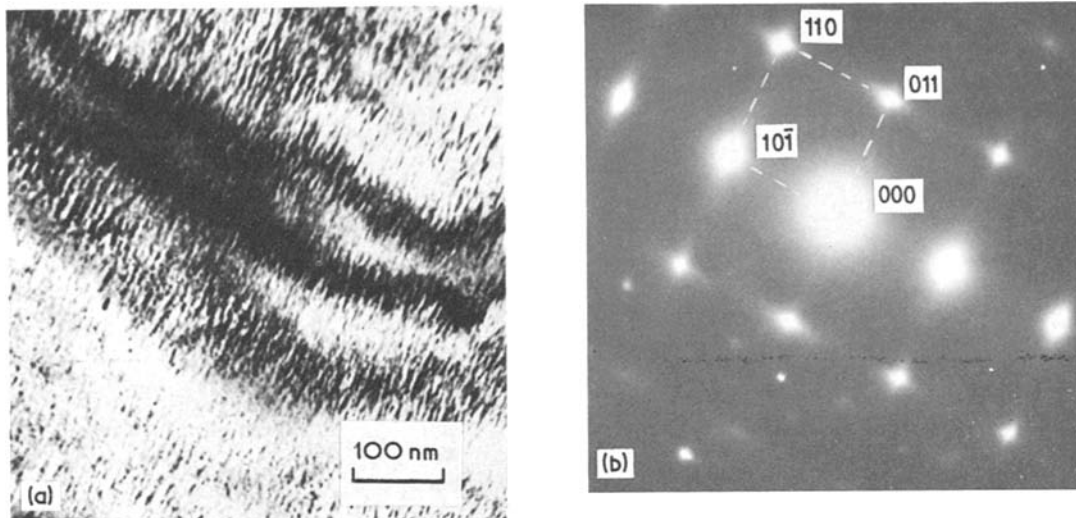


Figure 6 Microstructure of completely crystallized Te–20 at. % Pb alloy: (a) TEM micrograph, (b) selected area diffraction (SAD) pattern.

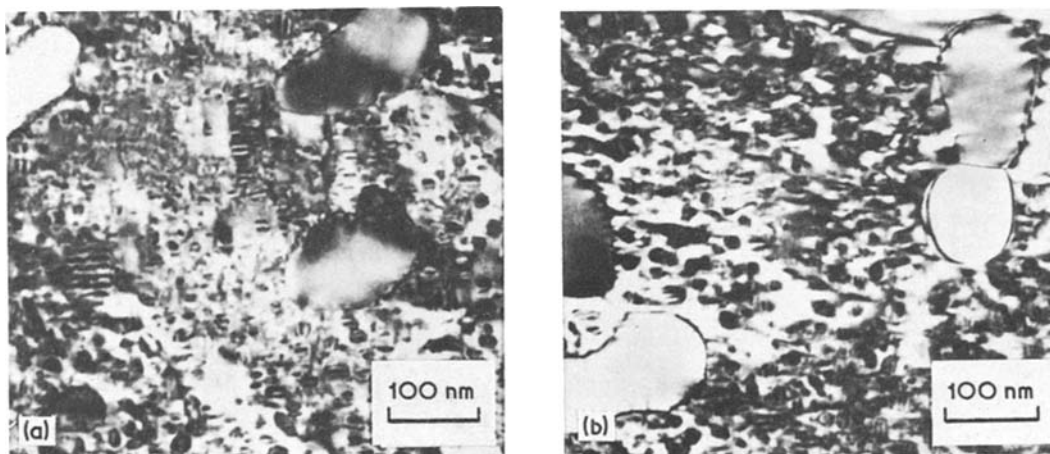


Figure 7 Microstructure of alloy after further beam heating: (a) small coherent precipitates of PbTe, (b) example of large incoherent precipitate of PbTe.

Fig. 8a shows the structure of the Te–20 at. % Pb alloy heated to a temperature at which partial melting of the foil has already occurred. Consistent with the electron diffraction pattern (Fig. 8b), the alloy has already attained its equilibrium structure, being a mixture of Te and PbTe crystals.

4. Discussion

According to the results of calorimetric, X-ray and electron microscopic studies, crystallization of amorphous Te–20 at. % Pb begins at 337 K. At this temperature, nucleation and growth of single crystals distributed at random within the amorphous matrix take place. This form of crys-

tallization can be regarded as indirect evidence for the genuinely amorphous structure of the material immediately after rapid cooling [14]. The strong thermal effect occurring within a narrow temperature range also confirms that the initial structure is amorphous (Fig. 3). Phase MS I formed during crystallization of amorphous alloy Te–20 at. % Pb is a Te(Pb) solution, which, as deduced from X-ray diffraction and electron diffraction studies, has a hexagonal structure with lattice parameters $a = 4.49 \text{ \AA}$ and $c = 5.85 \text{ \AA}$. An equivalent description of this structure on the basis of a primitive rhombohedral cell was suggested by Giessen [15]. Contrasts observed in the micrographs of single crystals

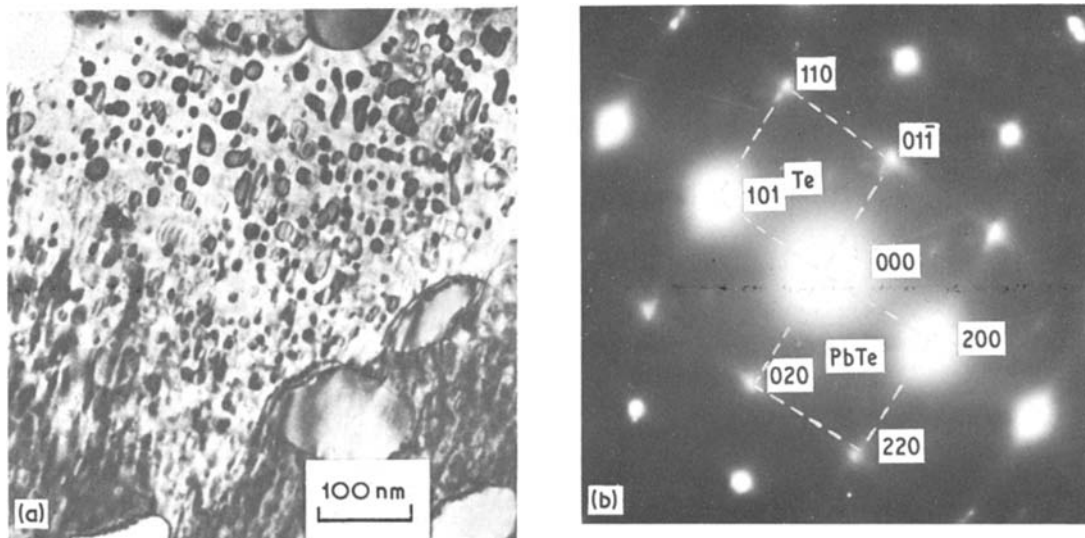


Figure 8 Equilibrium structure of alloy: (a) TEM micrograph, (b) SAD pattern (reflections from PbTe and from Te are clearly separated).

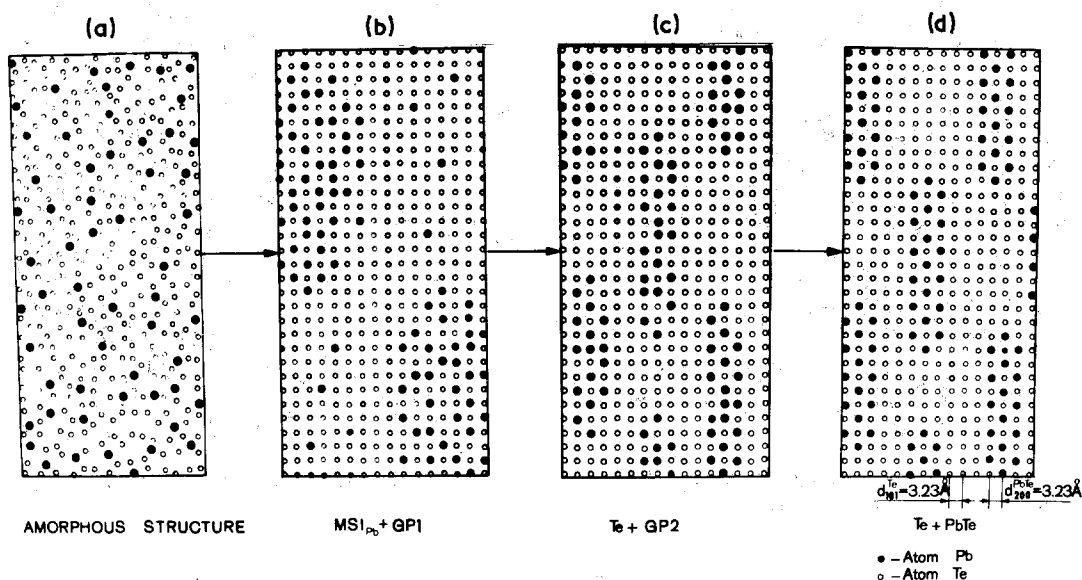


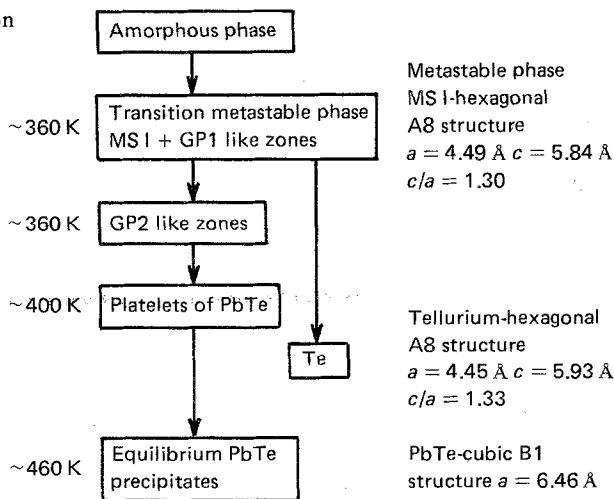
Figure 9 Two-dimensional model showing the successive stages of decomposition of the amorphous phase (dimensions of zones and distances between them are not to scale).

formed at the initial stage of crystallization (Figs. 4 and 5) are interpreted as effects related to the occurrence, within the grains of phase MS I, of areas with an increased Pb atom concentration. The fine striations can be regarded as zones analogous to GP zones; it seems that in this case they more closely approach the zones described by the Toman model, rather than the Gerold model [16]. Similar contrasts have been observed, among others, also by Fisher and Embury [17] in the

Au-20 at. % Ni alloy. Formation of a modulated substructure causes characteristic diffuseness of reflections in the electron diffraction patterns (magnified spot in corner of Fig. 4); according to Woodilla and Averbach [18], this diffuseness may point to a transition of the type of spinodal decomposition.

To explain how, during growth of the phase MS I crystals, areas with an increased lead atom concentration are formed, the following model is

Figure 10 Schematic diagram of the decomposition of amorphous phase in a Te–20 at.% Pb alloy.



proposed (Fig. 9). In the initial stage of crystallization of amorphous Te–20 at.% Pb (Fig. 9a) there is nucleation of the metastable intermediate phase MS I, which can be regarded as tellurium supersaturated with lead. During crystal growth the lead atoms, whose mean concentration in the amorphous phase is 20 at.%, come into contact with the growing crystal. Only a few of them can be absorbed by the crystalline phase, by occupying the nodes in the Te chains. The remaining Pb atoms become concentrated at the boundary between the growing crystal and the surrounding amorphous phase. With crystal growth, these atoms are “pushed” into the amorphous phase till they attain a certain critical concentration permitting steric configurations of the Te and Pb atoms in which each tellurium atom is surrounded by six lead atoms (Fig. 9b). On account of the attractive interactions between the Te and Pb atoms, these configurations can be fairly stable; being unable to diffuse as a whole inside the amorphous phase, they remain within the crystal of phase MS I. Many repetitions of the formation cycle of these zones may lead to the formation of the structure observed in the micrographs. Some doubts may be raised by the indispensable assumption of long-range diffusion of the “big” lead atoms ($r_{\text{Pb}} = 1.78 \text{ \AA}$), for the micrographs show that the length of the fluctuation wave, λ , is 80 \AA . This can be explained by the occurrence, in the amorphous phase, of a considerable number of vacancies, rendering diffusion less difficult. During further heating of the alloy, a “narrowing” of the areas with enhanced lead concentration takes place (Fig. 9c), this being expressed in sharpening of the

contrasts in the micrographs (Fig. 6a) and an increase in the diffuseness of the reflections in the diffraction patterns. Formation of these narrow zones, designated as GP2, causes considerable deformation of the atomic planes neighbouring with them. This results in the occurrence of characteristic strain contrasts, which are clearly visible in the micrographs (Fig. 6a). The direction of elongation of the nodes of the reciprocal lattice indicates that the smallest dimension of the zones is perpendicular to the planes of $\{101\}$ type of phase MS I. Further elevation of the temperature causes dissolution of GP 2 zones and the formation of platelet precipitates of PbTe compound (Fig. 9d). At the same time the MS I phase, owing to the loss via diffusion of the Pb atoms which supersaturate this phase, changes into Te. Precipitates of PbTe compound occur in the form of platelets, which are partly coherent with the matrix. This is testified to, *inter alia*, by the fact that 200 reflections originating from PbTe and 101 from Te are superimposed. Further heating of the foils causes coagulation of the precipitates, leading to a loss of coherence. This loss of coherence is accompanied by dislocations occurring at the interface between the precipitate and matrix, as well as by separation of 200_{PbTe} and 101_{Te} reflections (Fig. 8b).

The sequence of transitions taking place during continuous heating of amorphous alloy Te–20 at.% Pb can be presented in the form of the schema shown in Fig. 10.

Acknowledgement

We thank Professor N.J. Grant and Professor B.C. Giessen for helpful discussion and Dr H. Jones for

very valuable remarks. Thanks are also due to Dr M. Lasocka for her help with DSC analysis. This work was supported by U.S. National Science Foundation under Grant GF 42176.

References

1. H. L. LUO and P. DUWEZ, *Appl. Phys. Letters* **2** (1963) 21.
2. P. DUWEZ, *Trans. ASM* **60** (1967) 607.
3. C. C. TSUEI, *Phys. Rev.* **170** (1968) 775.
4. P. DUWEZ and C. C. TSUEI, *J. Non-Cryst. Sol.* **4** (1970) 345.
5. M. R. ANSEAU, *J. Appl. Phys.* **44** (1973) 3357.
6. M. LASOCKA, P. G. ZIELINSKI and M. MATYJA, *Scripta Met.* **9** (1975) 873.
7. T. TAKAMORI, R. ROY and G. J. MCCARTHY, *Mat. Res. Bull.* **7** (1970) 529.
8. M. LASOCKA and H. MATYJA, *Proceedings of the International Conference: "Physics of Non-Crystalline Solids IV"* 13–17 Sept. 1976 Clausthal, West Germany, (in press).
9. P. DUWEZ and R. H. WILLENS, *Trans. AIME* **227** (1963) 362.
10. P. CHAUDHARI, J. F. GRACZYK and S. R. HERD, *Phys. Stat. Sol. (b)* **51** (1972) 80.
11. S. R. HERD and P. CHAUDHARI, *Phys. Stat. Sol. (a)* **26** (1974) 627.
12. M. L. RUDEE, *Thin Sol. Films* **12** (1972) 207.
13. A. HOWIE, O. L. KRIVANEK and M. L. RUDEE, *Phil. Mag.* **27** (1973) 235.
14. P. DUWEZ in "Phase Stability in Metals and Alloys", edited by P. S. Rudman, J. Stringer and R. I. Jaffee (McGraw-Hill, New York, 1967) p. 523.
15. B. C. GIESSEN, Private communication (1975).
16. V. A. PHILIPS, *Acta Met.* **21** (1973) 291.
17. R. M. FISHER and J. D. EMBURY in "Electron Microscopy 1964", Vol. A, edited by M. Titlbach, (Czech. Academy of Science, Prague, 1964) p. 149.
18. J. E. WOODILLA and B. L. AVERBACH, *Acta Met.* **16** (1968) 255.

Received 10 May and accepted 27 May 1977.